# ON THE ROLE OF INFLOW TURBULENCE FOR MIXING IN A T-JUNCTION

**Eric Séverac**
Institut für Strömungsmechanik
Technische Universität Dresden
George-Bähr-Str. 3c
01062 Dresden, Germany
eric.severac@tu-dresden.de

**Robert Schadwill**
Institut für Strömungsmechanik
Technische Universität Dresden
George-Bähr-Str. 3c
01062 Dresden, Germany
robertschadwill@googlemail.com

**Jochen Fröhlich**
Institut für Strömungsmechanik
Technische Universität Dresden
George-Bähr-Str. 3c, 01062 Dresden, Germany
jochen.froehlich@tu-dresden.de

## ABSTRACT

Large Eddy Simulations are performed in a T-junction to analyze the influence of the turbulence level of the inlets on the thermal mixing inside the pipe in the framework of predicting the thermal fluctuations acting on the pipe walls due to turbulent mixing. The Smagorinsky model and the simplest temperature model are tested an a coarse mesh against existing experimental data. The influence of the turbulence is then investigated at lower Reynolds number with four simulations featuring a block profile at the two inlets, two fully turbulent pipe flow from separate "precurssor" simulations, one block profile for the main inlet and one precursor for the side inlet, and vice versa. It results that the turbulence level at the inlets has little influence on the mean flow in the core of the pipe, but a major inlfuence on the turbulence level close to the walls and inside the recirculation zone. This modify greatly the mixing process, changing the position of the mixing zone in the radial direction, and the global temperature mixing in the cross section. It is also to be reported that the two inlets do not have the same inluence and the mixing process is accelerated when the side inlet is more turbulent than the main inlet.

## INTRODUCTION

In power plants and other facilities dealing with high temperature differences a frequently occuring technological element is the T-junction, where hot fluid is injected into cold fluid, or vice versa. In this situation, flow instabilities and turbulent structures generate substantial temperature fluctuations at the inner wall of the pipe, which then induce thermal stress creating thermal fatigue, characterized by a deterioration of the material and possibly cracking. A key issue for thermal fatigue and lifespan are high frequencies of temperature fluctuations inside the pipe wall. These are, however, coupled with low frequencies inside the fluid as the difference of thermal conduction creates a low pass filter at the wall surface. Therefore, a better prediction of the unstewady structures in the turbulent flow and their impact on the heat transfer is of paramount importance.

Although the turbulence level of the inlet boundary condition is curtial in Direct Numerical Simulation and Large Eddy Simulation, the nature of the inflow is often disregarded in the numerical studies on T-junctions (Jayaraju *et al.*, 2010), as the strong large-scale instability in the mixing zone is triggered independently of the type of inflow conditions (Westin *et al.*, 2008). However the local mixing, particularly close to the wall can be influenced by the turbulence level at the inlet (Ndombo & Howard, 2011).

In the present study, a Large Eddy Simulation is performed for the experiment of Walker *et al.* (2009). Then, the turbulent inflow conditions are investigated in detail for each inflow plane separately to estimate their respective influence.

## METHOD AND CONFIGURATION

To carry out the present study, the code LESOCC2 (Hinterberger *et al.*, 2007), was used to solve the incompressible Navier-Stokes equations with a Large Eddy Simulation model and a scalar transport equation for the temperature. The subgrid-scale treatment was performed using the model of Smagorinsky (1963) with a constant $C_s = 0.1$ and damping close to the wall after Piomelli (1993). The geometry, presented in Fig. 1, consists of two pipes of the same diameter $D$ (radius $R = D/2$) in a perpendicular junction. The two inlets of the computational domain are placed $200\,mm$ upstream the center of the tee and the downstream pipe is $800\,mm$ long. The grid is multiblock-structured, using an O-grid topology for the pipes. The topology of the T-region is represented in Fig. 1. The wall-function of Werner & Wengle (1993) was employed for the velocity.

Two types of inflow conditions for the velocity are investigated here, a constant velocity at the inlet (block profile with $U_{in}(r,\phi,t) = U_b$, where $(r,\phi)$ is the local cylinder coordinate in a cross-section of the pipe) and a fully developed turbulent flow. The latter was computed separately with a so-called "precursor" simulation featuring a periodic pipe

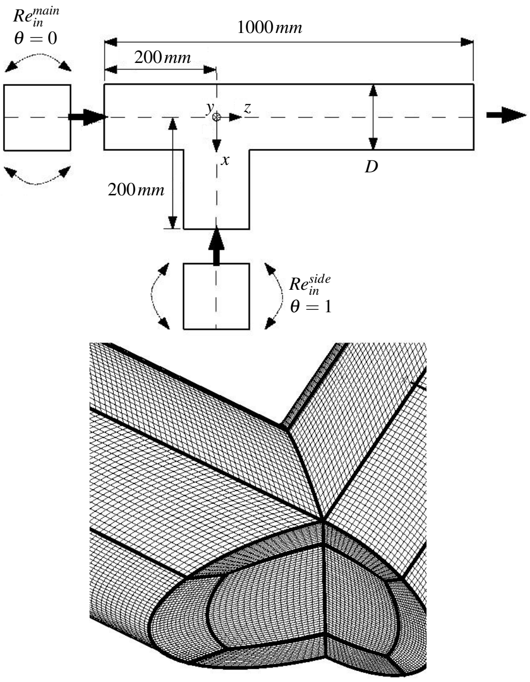


Figure 1. (Top) sketch of the geometry (not to scale). (Bottom) topology and grid size of the junction.

flow of same diameter as the tee and of length 200 $mm$. The profiles of the flow statistics at $1\,D$ upstream the tee for both inlets (precursor and block profile) are provided in Fig. 2. One can recognize that starting from a block profile inlet placed at $z = -3.4\,D$ upstream, the pipe flow has already started to develop and provides already a weak turbulence level close to the wall.

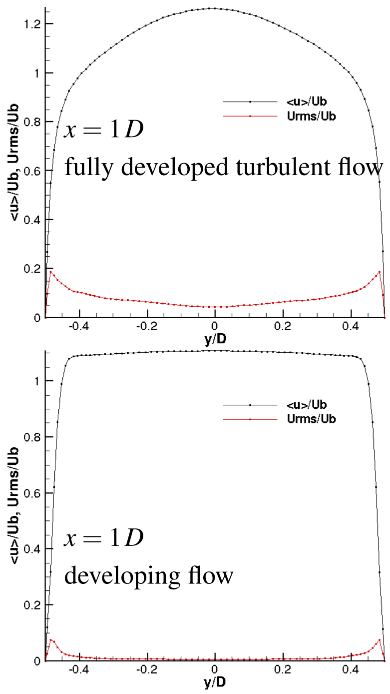


Figure 2. Profiles of the mean axial velocity $\langle u \rangle / U_b$ and its fluctuations $u_{rms}/U_b = \sqrt{\langle u'^2 \rangle}/U_b$ for the side inlet at $x = 1\,D$ when using the precurssor (top) and the block profile (bottom).

The simplest model for temperature is used, constant physical properties for the fluid, with $Pr = 8.44$, and constant turbulent Prandlt number, $Pr_t = 0.2$. The cold fluid being injected at the main inlet ($\theta = 0$) and the hot fluid at the side inlet ($\theta = 1$), where $\theta = (T - T_{cold})/(T_{hot} - T_{cold})$ is the dimensionless temperature. Adiabatic walls (zero-gradiant of temperature normal to the wall) are considered.

To mimic (Walker *et al.*, 2009), the same physical values are employed: $D = 0.51\,mm$, $U_b^{main} = 0.47\,m/s$, $U_b^{side} = 0.48\,m/s$ and $\nu = 1.18\,10^{-6}\,m^2/s$. The corresponding size of the cells at the wall toward the outlet ($Re_{in}^{main} = 20315$, $Re_{in}^{side} = 20745$ and $Re_{mix} = 41060$) is $r_1^+ = 8$, $R\Delta\phi^+ = 15$ and $\Delta z^+ = 20$. For this comparison, the influence of the turbulence level was not investigated, a single simulation with two precursors was computed. Also, the experiment (Walker *et al.*, 2009) was conducted with isothermal water, the mixing being measured with the difference of electrical conductivity between normal tap water at the side inlet and deionized water at the main inlet. These justify the temperature model carried on in this study.

To investigate the influence of the inflow turbulence on the mixing, a lower Reynolds number is chosen: $Re_{in}^{main} = 15000$, $Re_{in}^{side} = 15000$ and $Re_{mix} = 30000$. The corresponding size of the cells at the wall toward the outlet is $r_1^+ = 6$, $R\Delta\phi^+ = 11$ and $\Delta z^+ = 14$. Moreover, to emphasize the impact of the different inflow conditions, the modelisation of the temperature is slightly changed by fixing a constant boundary condition at the wall $\theta = 0$ and modelling the evolution of the temperature close to the wall with the wall-function of Kader (1981). Four simulations are performed to investigate separatly the impact of the turbulence at each inlet: one with block profiles at both inlets, one with precursors at both inlets, one with a block profile at the main inlet and a precursor at the side inlet, and vice-versa.

## COMPARISON WITH THE EXPERIMENTAL RESULTS

An impression of the instantaneous flow is provided by Fig. 3 showing the velocity in the main streamwise direction for the first case. One can recognize the characteristics of a

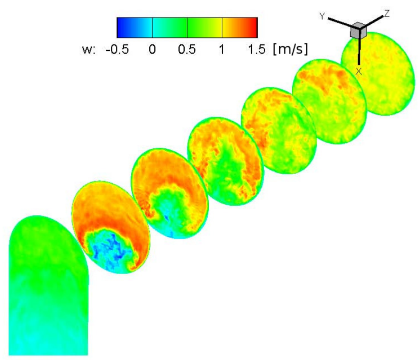


Figure 3. Contours of the instantaneous axial velocity $w$ for $z = 0, 1, \ldots, 6D$.

jet in crossflow but with the added constraint of being confined in the pipe. Due to the sharp corners of the tee, the side flow has a fixed separation on the upstream side of the pipe and creates a recirculation zone downstream of the tee with a length of around two diameters, while the main flow is pushed toward the opposite side of the incoming jet and accelerates. The velocity profile regularizes and is almost back to a standard pipe flow around six diameters downstream. In the study of Walker *et al.* (2009), "temperature" measurements were performed, but the velocity data generated suffer from substantial measurements errors (Walker & Prasser, 2012).

The hot fluid, coming from the sideflow, enters the recirculation zone so that the "temperature" in this region is elevated ($\theta \approx 1$), Fig. 4. In the present case, the mixing

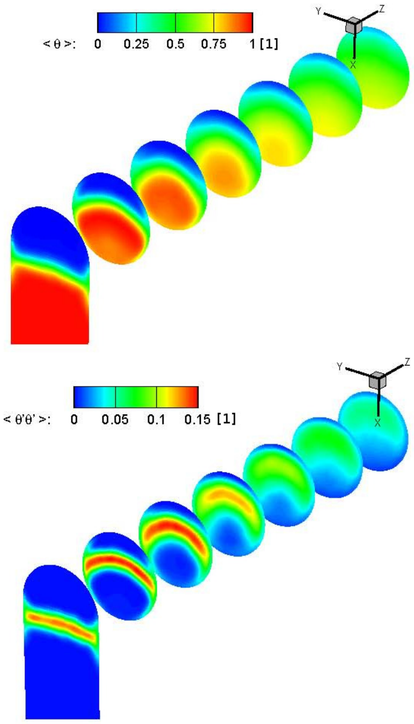


Figure 4. Contours of the mean temperature $\langle\theta\rangle$ and the temperature variance $\langle\theta'\theta'\rangle$ for $z = 0, 1, \ldots, 6D$.

layer is relatively stable (the separation point is fixed) so that the mixing starts weakly. Further downstream, the mixing zone widens and the temperature is almost uniform over the entire cross-section. At the lateral line where the mixing layer touches the wall, the increased turbulent kinetic energy of the inner layer enhances the transport of temperature along the wall in the azimuthal direction.

To assess the quality of the LES, profiles of the statistics of the temperature are compared, Fig. 5 and Fig. 6, at three axial positions downstream of the tee: inside the recirculation zone at $z = 1D$, at the end of the recirculation zone for $z = 2D$, and downstream of the recirculation at $z = 3D$.

The profiles of the mean temperature in Fig. 5 show that the size of the recirculation zone is not perfectly captured. Its radial extension is around $2\,mm$ ($0.04D$) larger in the LES at the axial position $z = 1D$ and moreover the profiles at $z = 2D$ presents a recirculation zone for the LES simulation but not anymore for the experimental results. Downstream of the recirculation at $z = 3D$ the quantitative agreement is quite good.

The profiles of the temperature variance in Fig. 6 are in acceptable agreement at $z = 1D$, aside from the $0.04D$ shift in radial position mentioned previously. Indeed, both the amplitude and the radial extension of the mixing are correctly captured. The profiles at $z = 2D$ corroborate the previous findings: this location is still inside the recirculation zone for the LES data (same amplitude of the variance $\langle\theta'\theta'\rangle^{LES}_{max} \approx 0.15$ and widening of the mixing layer), but in the experiment, the recirculation is shorter, so that this point is beyond its end (smaller amplitude of the variance $\langle\theta'\theta'\rangle^{Exp}_{max} = 0.13$ and wider profile than the LES).

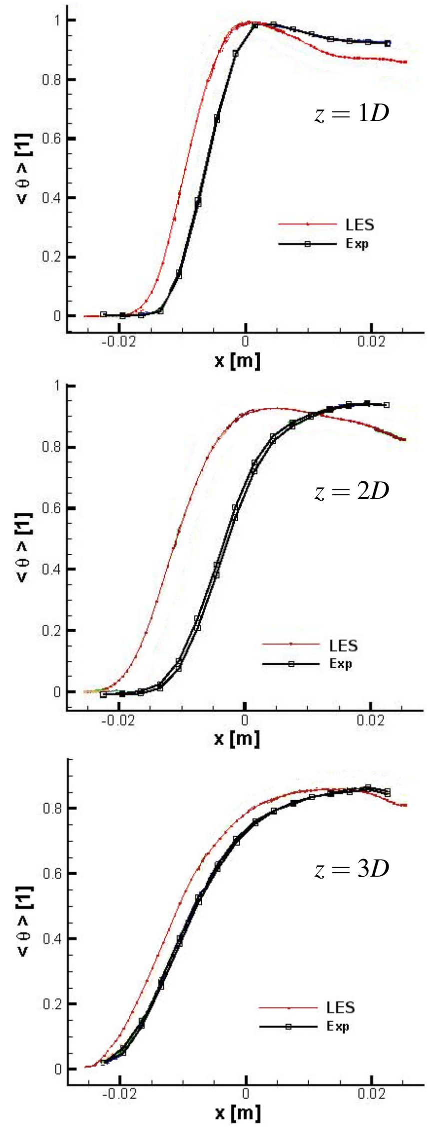


Figure 5. Profiles of the mean temperature $\langle\theta\rangle$ along a vertical line in the middle of the cavity. Comparison between the Experiment and the LES.

Downstream of the recirculation at $z = 3D$, the experimental profile has a surprising increase of magnitude to $\langle\theta'\theta'\rangle^{Exp}_{max} = 0.14$ when it should decrease, as found in LES with $\langle\theta'\theta'\rangle^{LES}_{max} = 0.12$. A grid study, not presented here, provided some improvement of the LES data, the major contribution being the resolution close to the wall and in the region where the recirculation occurs. However at this Reynolds number, the evolution of the viscous length is so important along the wall due to the acceleration of the main flow, that a good resolution would be very expensive for block-structured grids.

The time evolution of the mixing is closely compared by analyzing the spectrum of the fluctuations of temperature at the beginning of the mixing layer at the point $(x, y, z) = (-0.147D, 0, 1D)$ in Fig. 7. It appears that the low frequencies ($f \leq 10Hz$) and the medium frequencies ($10Hz \leq f \leq 100Hz$) are correctly captured by the LES. On the other hand, the higher frequencies ($100Hz \leq f$) are much more damped in the simulation. That is to be expected since the LES filters the small scales, responsible for the high frequencies of the flow. The underestimation of the higher frequencies, however, is not of importance for the current problematic as previous studies linked the thermal fatigue with the low frequencies of the flow though

International Symposium
On Turbulence and Shear Flow
Phenomena (TSFP-8)
August 28 - 30, 2013 Poitiers, France



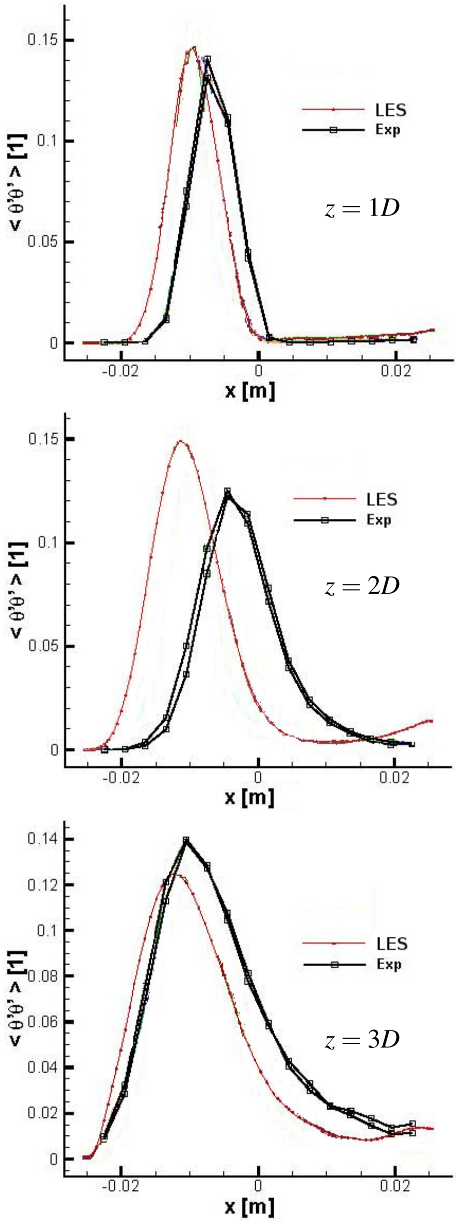


Figure 6. Profiles of the temperature variance $\langle \theta'\theta' \rangle$ along a vertical line in the middle of the cavity. Comparison between the Experiment and the LES.

the High Cycle Fatigue (HCF) and the very low frequencies ($f \leq 1\,Hz$) of the flow through the Low-Cycle Fatigue (LCF).

## INFLUENCE OF THE PRECURSORS ON THE MIXING

The profiles of the axial velocity in Fig. 8 display a recirculation zone after the tee in all configurations, only the case with block profile at both inlets yields a modification of the recirculation zone dowstream at $z = 1D$: the profile of the mean axial velocity presents a stagnation point within the recirculation zone. The corresponding turbulent kinetic energy, represented in Fig. 9, has two maxima: one in the mixing zone and one close to the wall, at the "stagnation" point mentioned previously. Also the maximum of the turbulent kinetic energy in the mixing zone is independent of the turbulence level at the inlet, an observation also made by Ndombo & Howard (2011) for a similar configuration.

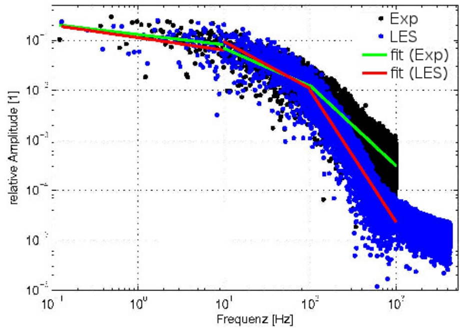


Figure 7. Temporal spectrum of the fluctuations of the temperature inside the mixing layer at $(x,y,z) = (-0.147D, 0, 1D)$. Comparison between the experiment and the LES.

Downstream of the recirculation zone at $z = 2D$ one can

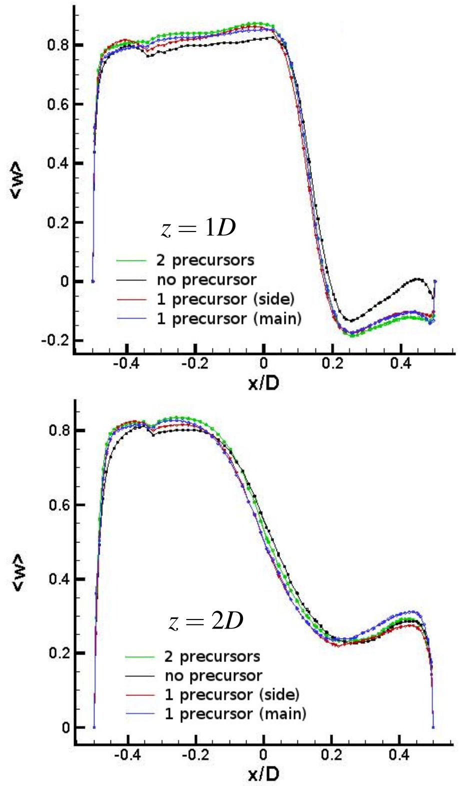


Figure 8. Profiles of the mean axial velocity $\langle w \rangle$.

notice that the mean flow is identical in all cases, but that the turbulent kinetic energy relaxes faster for the case with block profile at both inlets.

The profiles of the mean temperature in Fig. 10 and the temperature fluctuations in Fig. 11 provides noticeable differences between the four simulations in some key regions. More precisely, the level of turbulence at the inlet modify the radial position of the mixing zone and the mean temperature on the side of the recirculation zone. The case with two block profiles at the inlets presents a broad region of constant temperature on the side of the recirculation zone at $z = 2D$ in Fig. 10, while the three other cases present a maximal mean temperature toward the center of the pipe and a slow decrease of mean temperature toward the wall on the side of the recirculation. Also, the mixing zone is shifted toward the center of the pipe in the case with two block profile at the inlets.

Further downstream, the profiles at $z = 4D$, show that although the total fluctuations of temperature are not dependent on the turbulence level at the inlets, the mean temperature profile downstream the recirculation zone depends

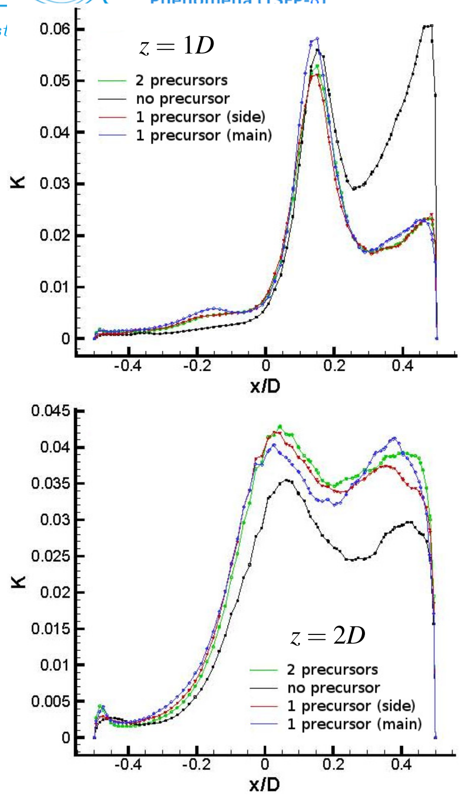


Figure 9. Profiles of the turbulent kinetic energy $K = \frac{1}{2}\left(\langle u'^2\rangle + \langle v'^2\rangle + \langle w'^2\rangle\right)$.

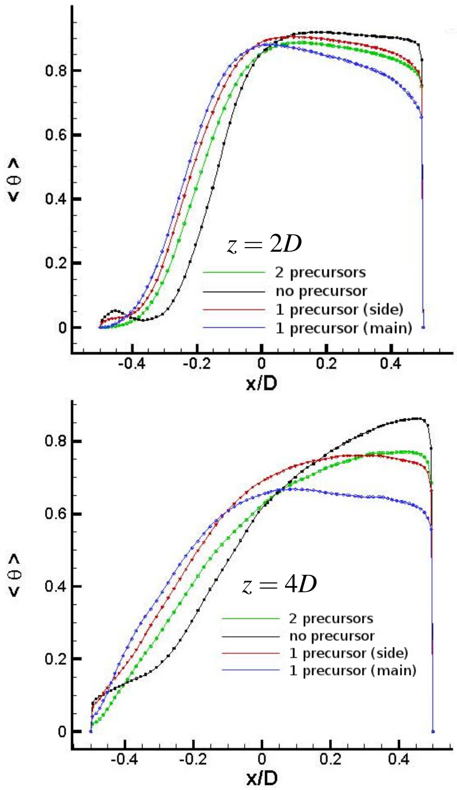


Figure 10. Profiles of the temperature average $\langle\theta\rangle$.

on the turbulence level of the inlets. More precisely, the highest value of $\Delta\theta = \langle\theta\rangle_{max} - \langle\theta\rangle_{min}$ is lower for the case with constant velocity at both inlets, which show that the total dispersion of temperature between the tee and $z = 4D$ is lower. But on the other hand, the lowest value of $\Delta\theta$ is obtained for the case with turbulence only on the main inlet. This profile also shows a larger plateau of maximal mean temperature on the same side than the side inlet, which means that although the dispersion was larger inside the mixing zone, the dispersion is much weaker afterward.

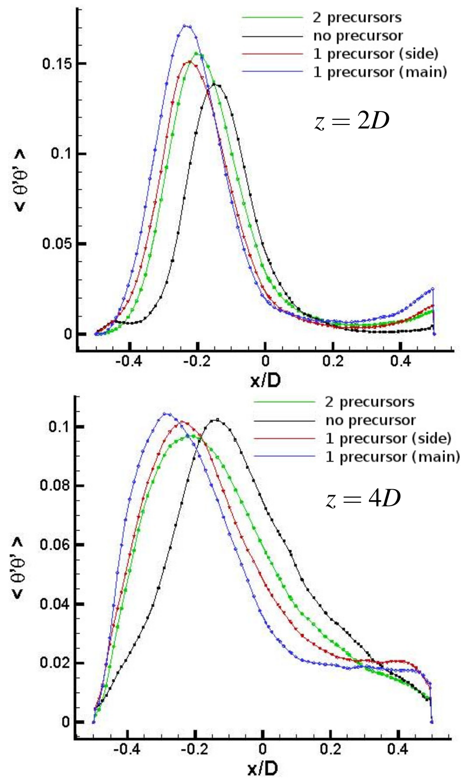


Figure 11. Profiles of the temperature variance $\langle\theta'\theta'\rangle$.

The fluctuations in Fig. 11 corroborate the previous findings at $z = 2D$: the lower the fluctuations in the mixing zone, the more the latest is shifted toward the center of the pipe. However further downstream at $z = 4D$, all cases present a maximum of fluctuation almost identical even though the shift remains. Specifically, the case with block profile at both inlets displays consistantly a maximum of fluctuation farther away from the wall.

## CONCLUSIONS

The influence of the inlet turbulence on the mixing process of a T-junction has been analysed by mean of Large Eddy Simulation. Two types of inlet has been considered, one with a velocity equal to the bulk velocity placed $\approx 4D$ upstream the tee, and one with a fully developed turbulent pipe flow out of a so-called "precursor" simulation. The results have been compared with the experiments of Walker *et al.* (2009) for high Reynolds number, low Froude number, adiabatic walls and same velocity ratio at the inlet.

In agreement with (Ndombo & Howard, 2011), the present results do not reveal an influence of the turbulence level at the inlet on the mean velocity field, but on the turbulent kinetic energy along the wall downstream of the T-junction on the side of the side-inlet. The decrease of turbulence at the inlet changes, however, the mean temperature distribution by either creating large zones without mixing or decreasing the overall dispertion of the temperature, the larger influence being noticed close to the wall. Inside the core of the flow, the temperature fluctuations respond to a decrease of turbulence at the inlet by shifting its maximum toward the center of the pipe.

Also, the results of the case with a fully turbulent pipe flow at the side inlet and a constant velocity at the main inlet are close of the results with two precursors. This hints toward an unequal influence of the turbulence level between the two inlets, a side inlet more turbulent than the main inlet favoring the mixing.

In regards of the thermal fatigue, the temperature fluctuations at the wall is of most interest. As both this present study and the one of Ndombo & Howard (2011) have shown, the turbulence level at the inlets of a T-junction has most influence close to the wall on the intensity of the turbulence. A feature that requires further study with more effort on the wall-resolution (including a coupled heat transfer between the fluid and a solid pipe wall) and finer tools to analyse not only the temperature statistics but also the frequencies (especially the low ones) of the velocity and temperature fluctuations.

## ACKNOWLEDGEMENTS

The present work was funded by $e \cdot on$ through the project MOTHER (EDF *et al.*, 2012). Computing time was provided by ZIH Dresden. The authors thank R.J.A. Howard of EDF for valuable discussions on the topic.

## REFERENCES

EDF, Vattenfall R&D, $e \cdot on$, AREVA, CEA, PSI, NRG, TU Dresden, Onsala & SPG 2012 MOdelling T-junction Heat transfER (MOTHER) - a project in the NULIFE framework portfolio. CONSORTIUM AGREEMENT number 8610-AAP-5910083925.

Hinterberger, C., Fröhlich, J. & Rodi, W. 2007 Three-dimensional and depth-averaged large-eddy simulations of some shallow water flows. *Journal of Hydraulic Engineering* **133**, 857–872.

Jayaraju, S.T., Komen, E.M.J. & Baglietto, E. 2010 Suitability of wall-functions in Large Eddy Simulation for thermal fatigue in a T-junction. *Nuclear Engineering and Design (NED)* **240** (10), 2544–2554.

Kader, B.A. 1981 Temperature and concentration profiles in fully turbulent boundary layers. *International Journal of Heat and Mass Transfer* **24** (9), 1541 – 1544.

Ndombo, J.-M. & Howard, R.J.A. 2011 Large Eddy Simulation and the effect of the turbulent inlet conditions in the mixing Tee. *Nuclear Engineering and Design (NED)* **241**, 2172–2183.

Piomelli, U. 1993 High Reynolds number calculations using the dynamic subgrid-scale stress model. *Physics of Fluids* **A 5**, 1484–1490.

Smagorinsky, J. 1963 General circulation experiments with the primitive equations. *Monthly Weather Review* **91**, 99–164.

Walker, C. & Prasser, H.-M. 2012 privat communications.

Walker, C., Simiano, M., Zboray, R. & Prasser, H.-M. 2009 Investigations on mixing phenomena in single-phase flow in a T-junction geometry. *Nuclear Engineering and Design (NED)* **239**, 116–126.

Werner, H. & Wengle, H. 1993 Large-eddy simulation of turbulent flow over and around a cube in a plane channel. In *Selected Papers from the 8th Symposium on Turbulent Shear Flows* (ed. F. Durst, R. Friedrich, B. E. Launder, F. W. Schmidt, U. Schumann & J. H. Whitelaw), pp. 155–168. Springer.

Westin, J., Veber, P., Andersson, L., Mannetje, C., Andersson, U., Eriksson, J, Alavyoon, F. & Andersson, C. 2008 High-Cycle Thermal Fatigue in mixing tees. Large-Eddy Simulations compared to a new validation experiment. In *16th Int. Conf. On Nuclear Engineering (ICONE-16)*, pp. 1–11. Florida, Orlando, USA, 11-15 May 2008.